Symmetry energy from neutron-rich fragments in heavy-ion collisions, and its dependence on incident energy, and impact parameters *

MA Chun-Wang(马春旺)[1;1)] SONG Heng-Li(宋恒利)[1] PU Jie(普洁)[1,2] ZHANG Tong-Lin(张同林)[1,2]
ZHANG Sha(张莎)[1] WANG Shan-Shan(王闪闪)[1] ZHAO Xin-Li(赵新丽)[1] CHEN Li(陈丽)[1]

[1] Department of Physics, Henan Normal University, Xinxiang 453007, China
[2] Department of Nuclear Physics, Shanghai Institute of Applied Physics, Shanghai 201800, China

Abstract: The yields of fragments produced in the ^{60}Ni+^{12}C reactions at 80 A and 140 A MeV, and with maximum impact parameters of 1.5, 2 and 7.3 fm at 80 A MeV are calculated by the statistical abrasion-ablation model. The yields of fragments are analyzed by the isobaric yield ratio (IYR) method to extract the coefficient of symmetry energy to temperature ($a_{\rm sym}/T$). The incident energy is found to influence $a_{\rm sym}/T$ very little. It's found that $a_{\rm sym}/T$ of fragments with the same neutron-excess $I=N-Z$ increases when A increases, while $a_{\rm sym}/T$ of isobars decreases when A increases. The $a_{\rm sym}/T$ of prefragments is rather smaller than that of the final fragments, and the $a_{\rm sym}/T$ of fragments in small impact parameters is smaller than that of the larger impact parameters, which both indicate that $a_{\rm sym}/T$ decreases when the temperature increases. The choice of the reference IYRs is found to have influence on the extracted $a_{\rm sym}/T$ of fragments, especially on the results of the more neutron-rich fragments. The surface-symmetry energy coefficient ($b_{\rm s}/T$) and the volume-symmetry energy coefficient ($b_{\rm v}/T$) are also extracted, and the $b_{\rm s}/b_{\rm v}$ is found to coincide with the theoretical results.

Key words: symmetry energy, isobaric yield ratio, neutron-rich nucleus, heavy-ion collisions

PACS: 21.65.Cd, 21.65.Ef, 21.10.Gv **DOI:** 10.1088/1674-1137/37/2/024102

1 Introduction

Compared with the stable nucleus, the symmetry energy of the neutron-rich nucleus is less known, while it is important not only in nuclear physics, but also in some processes of astrophysics [1–5]. Depending on both density and temperature, symmetry energy of nuclear matter of super-saturation and sub-saturation density, and non-zero temperature are unclear theoretically. One main goal of developing radioactive nuclear beams is to study the properties of isospin asymmetric matter [6]. More efforts have been stimulated to extract the symmetry energies of hot emitting sources using the fragment distribution in heavy-ion collisions (HIC) [7–13].

The symmetry energy of the isospin symmetric fragment produced in the intermediate energy HIC has been extracted using the isobaric yield ratio (IYR) method [14–16] in the framework of a modified Fisher model (MFM) [7, 17, 18]. In the isoscaling method [8], the free energy of a fragment in reactions induced by the projectile of different isospin cancels out and only the chemical potentials of the proton and neutron are reserved. While in the IYR method, the free energy (which can be replaced by binding energy) of a fragment is kept and the symmetry energy of the fragment can be analyzed specifically.

In a previous work studying the isospin dependence of fragment production in the intermediate energy HIC, the ^{60}Ni+^{12}C reactions have been calculated using the statistical abrasion-ablation (SAA) model [19]. Since the SAA model can well reproduce the yields of fragments in intermediate energies HIC [13, 20–23], the results of ^{60}Ni+^{12}C reactions in Ref. [19] will be analyzed using the IYR method to extract the symmetry energy of a neutron-rich fragment.

2 Model description

2.1 Isobaric yield ratio and symmetry energy in modified Fisher model

In the modified Fisher model, the free energy of a fragment produced in HIC is linked to its yield [17, 18]. For a fragment with mass A and neutron excess $I=N$–Z,

Received 27 March 2012

* Supported by National Natural Science Foundation of China (10905017), Program for Innovative Research Team (in Science and Technology) in the Universities of Henan Province (2010IRTSTHN002) and Young Teacher Project in Henan Normal University

1) E-mail: machunwang@126.com

its yield ($Y(A,I)$) is given by

$$Y(A,I) = CA^{-\tau}\exp\{[W(A,I)+\mu_{\rm n}N+\mu_{\rm p}Z]/T + N\ln(N/A)+Z\ln(Z/A)\}, \tag{1}$$

where C is a constant. The $-\tau$ are identical for all fragments. $\mu_{\rm n}$ and $\mu_{\rm p}$ are the neutron and proton chemical potential, respectively, and $W(A,I)$ is the free energy of the cluster at temperature T, which is equivalent to the binding energy of a fragment [18]. Using the semiclassical mass formula [24, 25] at given temperature T and density ρ:

$$W(A,I) = -a_{\rm sym}(\rho,T)I^2/A - a_{\rm c}(\rho,T)Z(Z-1)/A^{1/3} + a_{\rm v}(\rho,T)A - a_{\rm s}(\rho,T)A^{2/3} - \delta(N,Z), \tag{2}$$

where the indexes v, s, c and sym represent coefficients of the volume-, surface-, Coulomb-, and symmetry- energy , respectively. The coefficients depend on T, which has a contribution from entropy [18]. To simplify the description, the density and temperature dependence of the coefficients in Eq. (2) are written as $a_{\rm i}=a_{\rm i}(\rho,\ T)$ (i= v, s, c, sym).

The isobaric yield ratio between the isobars differing by 2 units in I is defined as,

$$\begin{aligned} R(I+2,I,A) &= Y(A,I+2)/Y(A,I) \\ &= \exp\{[W(I+2,A)-W(I,A)+(\mu_{\rm n}-\mu_{\rm p})]/T \\ &\quad + S_{\rm mix}(I+2,A)-S_{\rm mix}(I,A)\}, \end{aligned} \tag{3}$$

where $S_{\rm mix}(I,A)=N\ln(N/A)+Z\ln(Z/A)$.

Inserting Eq. (2) into Eq. (3), and taking the logarithm of the resultant equation, one has,

$$\begin{aligned} \ln[R(I+2,I,A)]-\varDelta_I &= [(\mu_{\rm n}-\mu_{\rm p})-4a_{\rm sym}(I+1)/A \\ &\quad +2a_{\rm c}(Z-1)/A^{1/3} \\ &\quad -(sgn)2a_{\rm p}/A^{1/2}]/T, \end{aligned} \tag{4}$$

where $\varDelta_I=S_{\rm mix}(I+2,A)-S_{\rm mix}(I,A)$. Eq. (4) takes the assumption that $a_{\rm s}$ and $a_{\rm v}$ for isobars are the same. $a_{\rm p}$ has a form according to Ref. [26]. For odd-even nuclei (sgn)=0.

For mirror nuclei, $\varDelta_{-1}$=0, one gets

$$\ln[R(1,-1,A)]=[\Delta\mu+2a_{\rm c}(Z-1)/A^{1/3}]/T, \tag{5}$$

μ/T and $a_{\rm c}/T$ of mirror nuclei can be extracted from Eq. (5).

Taking the mirror nuclei as the references, i.e., replacing the $[\Delta\mu+2a_{\rm c}(Z-1)/A^{1/3}]/T$ term for isobars with I by the IYR of mirror nuclei, inserting Eq. (5) into Eq. (4),

$$\frac{a_{\rm sym}}{T} = \frac{A}{4(I+1)}\{\ln[R(1,-1,A)]-\ln[R(I+2,I,A)] - a_{\rm c}(I+1)/(A^{1/3}T)+\varDelta_I\}. \tag{6}$$

Taking the IYR of the neighboring I–2 isobars as the references, from Eq. (4) one obtains,

$$\frac{a_{\rm sym}}{T} = \frac{A}{8}\Big\{\ln[R(I,I-2,A)]-\ln[R(I+2,I,A)] - 2a_{\rm c}/(A^{1/3}T)-\varDelta_{I-2}+\varDelta_I\Big\}. \tag{7}$$

Using Eqs. (6) and (7), and adopting $a_{\rm c}/T$ of the mirror nuclei, $a_{\rm sym}/T$ of neutron-rich fragments can be extracted.

2.2 The statistical abrasion-ablation model

The SAA model was developed by Brohm and Schmidt to describe the relativistic energy HIC [27, 28] and modified by Fang et al. to describe the intermediate energy collisions [13, 20–23, 29–33]. In particular, the 140 A MeV ^{40,48}Ca and ^{58,64}Ni projectile fragmentation reaction have been calculated and it is found that the SAA model can well reproduce the yields both of the small and large mass fragments [23]. Here only some important formulae in SAA are listed since it is well described in Refs. [22, 23, 27, 28, 32].

In the SAA model, the colliding nuclei are described as being composed of parallel tubes orienting along the beam direction. Neglecting the transverse motion, the collision is described by independent interactions of tube pairs. Assuming a binomial distribution for the absorbed projectile neutrons and protons in the interaction of a specific pair of tubes, the distributions of the total abraded neutrons and protons can be determined. For an infinitesimal tube in the projectile, the transmission probabilities for neutrons (protons) at a given impact parameter $\vec{b}$ are calculated by

$$t_{\rm k}(\vec{s}-\vec{b})=\exp\{-[D_{\rm n}^{\rm T}(\vec{s}-\vec{b})\sigma_{\rm nk}+D_{\rm n}^{\rm P}(\vec{s}-\vec{b})\sigma_{\rm pk}]\}, \tag{8}$$

where $D^{\rm T}$ is the nuclear-density distribution of the target integrated along the beam direction and normalized by $\int{\rm d}^2sD_{\rm n}^{\rm T}=N^{\rm T}$ and $\int{\rm d}^2sD_{\rm p}^{\rm T}=Z^{\rm T}$. With $N^{\rm T}$ and $Z^{\rm T}$ referring to the neutron and proton number in the target respectively, the vectors $\vec{s}$ and $\vec{b}$ are defined in the plane perpendicular to the beam, and $\sigma_{\rm k'k}$ is the free nucleon-nucleon reaction cross section [34]. The average absorbed mass in the limit to infinitesimal tubes at a given $\vec{b}$ is

$$\langle\Delta A(b)\rangle = \int{\rm d}^2sD_{\rm n}^{\rm T}(\vec{s})[1-t_{\rm n}(\vec{s}-\vec{b})] + \int{\rm d}^2sD_{\rm p}^{\rm P}(\vec{s})[1-t_{\rm p}(\vec{s}-\vec{b})]. \tag{9}$$

The cross section for a specific isotope can be calculated from

$$\sigma(\Delta N,\Delta Z)=\int{\rm d}^2bP(\Delta N,b)P(\Delta Z,b), \tag{10}$$

where $P(\Delta N, b)$ and $P(\Delta Z, b)$ are the probability distributions for the abraded neutrons and protons at a given impact parameter b, respectively.

The second stage of the reaction is characterized by the evaporation of particles, which in the SAA model is described by the conventional statistical model under the assumption of thermal equilibrium in the excited prefragment. The excitation energy of the projectile spectator is estimated by a simple relation of $E^{*}=13.3\langle\Delta A(b)\rangle$MeV, where 13.3 is the mean excitation energy due to an abraded nucleon from the initial projectile [28]. After the de-excitation process, the yield of fragment which is comparable to the experimental result is obtained.

The secondary decay process greatly influences the yields of fragments, thus it affects the IYR and the resultant symmetry energy of fragment in the IYR methods [14], which is similar to the symmetry energy extracted by the isoscaling methods and other methods [12]. The IYRs for the prefragments produced right after the first-stage collisions will also be investigated.

3 Results and discussion

The cross sections of the prefragments (PFs) and final fragments (FFs) produced in the 80 A and 140 A MeV ^{60}Ni+^{12}C reactions calculated by the SAA model are plotted in Fig. 1. When $I<7$, the cross sections of PFs in the 80 A and 140 A MeV reactions have large difference when $A<30$. The cross sections of FFs in the 80 A and 140 A MeV reactions are similar to the PFs. The very neutron-rich PFs ($I>9$) no longer exist in FFs, which decay to smaller I fragments. The large difference between the cross sections of PFs and FFs suggests that the neutron-rich PFs can hardly survive the de-excitation process and decay to smaller A fragments with less neutron-richness.

The IYRs in the form of $[\ln R(I+2,I,A)-\Delta_I]$ for the PFs and FFs in the 80 A and 140 A MeV ^{60}Ni reactions are plotted in Fig. 2. The difference between the IYRs for PFs of each I group in the 80 A and 140 A MeV reactions are very small, but the difference increases when I becomes larger. The same status happens in the FFs in the 80 A and 140 A MeV reactions, and there are some obvious fluctuations. The IYRs for PFs in each I group form a plateau and the mean value of the plateau decreases very little when I increases. Generally, the IYRs for FFs of each I group increase when A becomes larger. But the IYRs for the isobars with different I decrease when I increases.

The a_{sym}/T of PFs and FFs produced in the 80 A and 140 A MeV ^{60}Ni+^{12}C reactions are plotted in Fig. 3. The labels (a) and (b) represent the results using Eq. (6) and Eq. (7), respectively. The $\ln[R(1,-1,A)]$ of fragments in the measured 40 A MeV ^{64}Zn+^{112}Sn reactions [14] are plotted as stars, which are similar to the calculated results. Generally, the a_{sym}/T of PFs are rather smaller

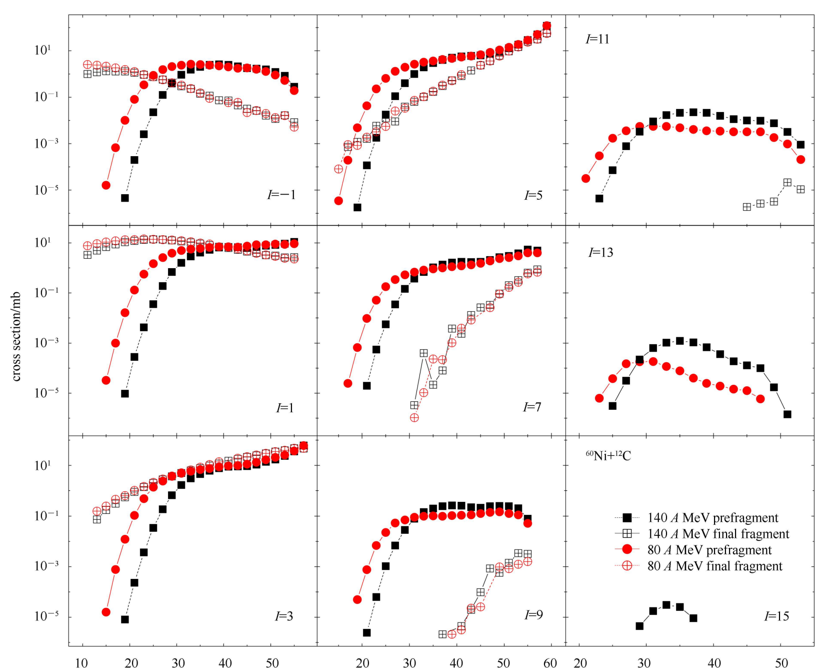

Fig. 1. (color online) The cross sections (in mb) of prefragments and final fragments in the 80 A and 140 A MeV ^{60}Ni+^{12}C reactions. The full and open symbols are for the prefragments and final fragments, respectively. The squares and circles are for the 140 A and 80 A MeV, respectively. The fragments are sorted as their neutron excess $I=N-Z$. The lines are just for guiding the eyes.

than those of the FFs, but the difference between $a_{\rm sym}/T$ of PFs and FFs becomes smaller when I increases. In the first collision stage when the PFs are produced, the temperature is high. The large mass PFs are produced in the peripheral reactions, which also correspond to low temperature. But the FFs are finally formed at low temperature from the de-excited PFs. This explains the decreasing difference between $a_{\rm sym}/T$ of the more neutron-rich PFs and FFs. The results suggest that $a_{\rm sym}/T$ of a fragment decreases when the T increases, which is coincident with the conclusion in Ref. [35].

The $a_{\rm sym}/T$ of PFs and FFs generally increase as A increases for each I group. For PFs, $a_{\rm sym}/T$ increases very slowly when $A<40$ and then increases faster. For FFs, $a_{\rm sym}/T$ increases from ∼5 to 20 very fast and saturates. But for FFs, $a_{\rm sym}/T$ of isobars decrease when

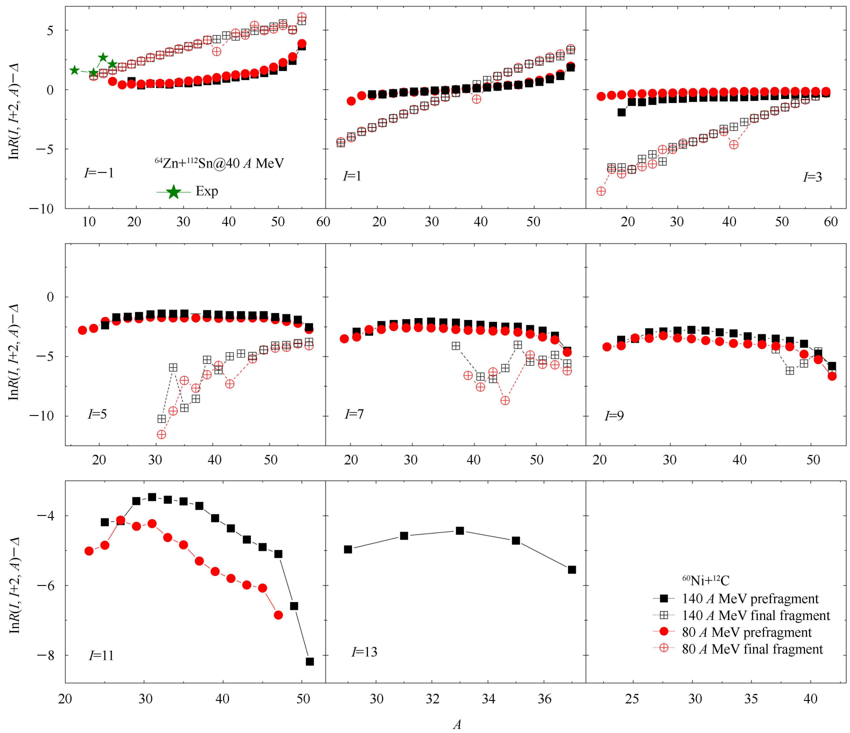

Fig. 2. The isobaric yield ratios [in the form of $\ln R(I,I+2,A)-\Delta$] for the PFs and FFs produced in the 80 A and 140 A MeV ^{60}Ni+^{12}C reactions. The different filling of symbols represents different I of fragments. The stars represent the $\ln[R(1,-1,A)]$ of the measured 40 A MeV ^{64}Zn+^{112}Sn reactions [14].

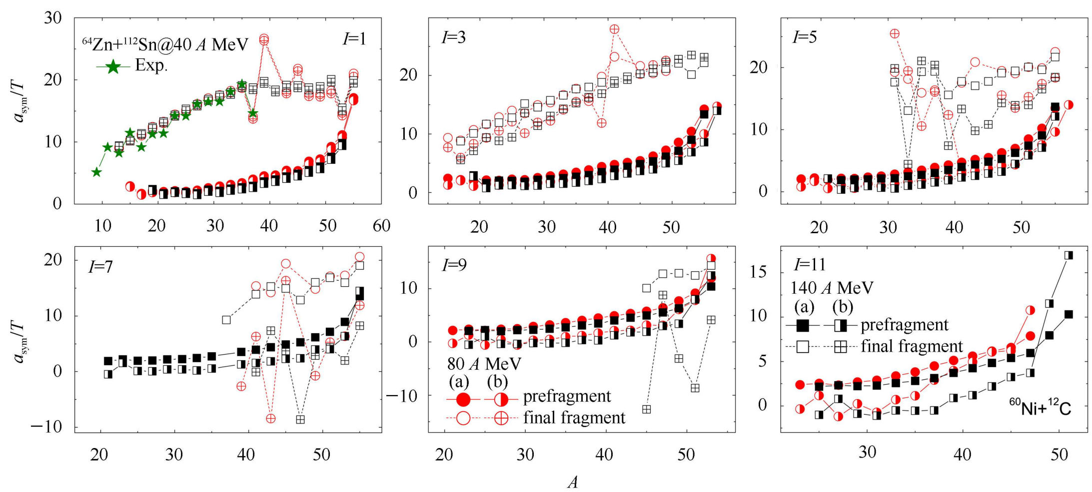

Fig. 3. The $a_{\rm sym}/T$ of PFs and FFs produced in the 80 A and 140 A MeV ^{60}Ni+^{12}C reactions. (a) and (b) represent the results using Eqs. (6) and (7), respectively. The stars represent the $a_{\rm sym}/T$ of the I=1 fragments in the measured 40 A MeV ^{64}Zn+^{112}Sn reactions [14].

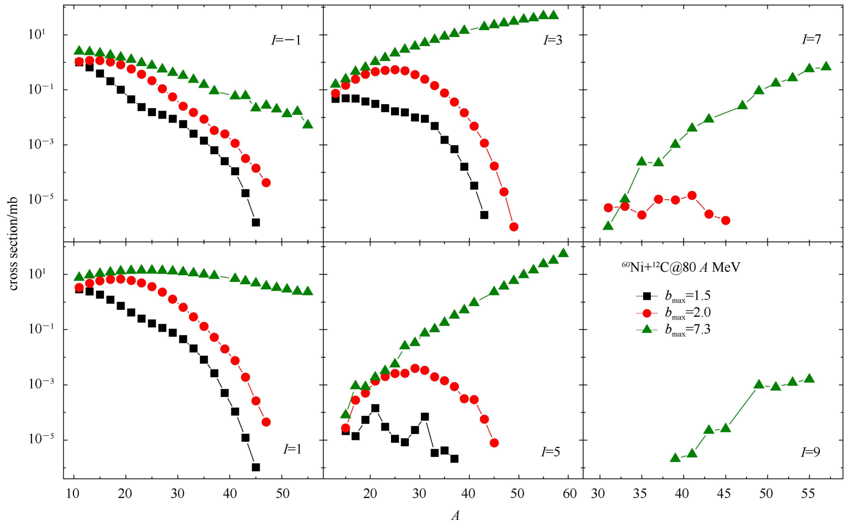

Fig. 4. The cross sections (in mb) of the final fragments produced in the 80 A MeV ^{60}Ni+^{12}C reactions calculated using the SAA model with different limitations on impact parameter ($b_{\max}$). The results with $b_{\max}$=1.5, 2.0 and 7.3 fm are plotted as squares, circles, and triangles, respectively. The fragments are sorted as their neutron excess I. The lines are just for guiding the eyes.

the mass becomes larger. The incident energy differences of 80 A and 140 A MeV have a larger influence on $a_{\rm sym}/T$ of PFs than those of FFs. The difference between the $a_{\rm sym}/T$ of PFs at 80 A and 140 A MeV is very little but it increases when I becomes larger. But generally, the incident energies of 80A and 140 A MeV do not influence $a_{\rm sym}/T$ very much.

The $a_{\rm sym}/T$ of the $I=1$ fragments in the 40 A MeV ^{64}Zn+^{124}Sn reaction [14] are also plotted as stars in Fig. 3. Though the incident energies of these reactions are not the same, the difference between the experimental and SAA calculated $a_{\rm sym}/T$ of the $I=1$ fragments has very little difference. The temperature evolution in the 26 A, 35 A, and 47 A MeV ^{64}Zn and ^{92}Mo reactions simulated by the AMD model reveals that the cooling and expansion periods for all three projectile energies are very similar, which indicates that hot nuclei with similar properties are produced [36]. The $a_{\rm sym}/T$ of fragments in the 80 A and 140 A MeV reactions calculated by the SAA model have very little difference, and very little difference between the 40 A MeV ^{64}Zn+^{112}Sn reactions is found. It's believable that in the fermi energy, $a_{\rm sym}/T$ of fragments obtained from HIC may be very similar.

In studying the influence of impact parameters on the yield of fragments, two limitations to the maximum of impact parameter are adopted, i.e., $b_{\max}$=1.5 and 2 fm, which all correspond to the central collisions (which are smaller than 30% of $1.17(A_{\rm p}^{1/3}+A_{\rm t}^{1/3})\approx7.3$) [19]. In Fig. 4, the cross sections of the FFs with different $b_{\max}$ in the 80 A MeV ^{60}Ni+^{12}C reactions are plotted. The cross sections of FFs increase as $b_{\max}$ increases from 1.5 to 7.3 fm. It's easy to see that the large A fragments and the very neutron-rich fragments are produced in the peripheral collisions, while the small A and the relatively n/p symmetric fragments are produced both in central and semi-central collisions. In particular, the cross sections of FFs first increase as A increases to a certain value and then decrease for $b_{\max}$=1.5 fm. The relatively small difference between cross sections of $A<25$ fragments for $b_{\max}$=2.0 and 7.3 fm suggests that they are mostly produced in the central and semi-central collisions. Combing the message from Fig. 1, the cross sections of $A<25$ fragments are greatly influenced by the de-excitation process.

The IYRs for FFs in the reactions with different $b_{\max}$ are plotted in Fig. 5. For fragments of each I, the IYRs for FFs of $b_{\max}$=1.5, 2 and 7.3 fm overlap when A of fragment is small. The difference is mainly between the large A fragments, which corresponds to the low production of large A fragments in central collisions. The values for IYRs between isobars decrease as I increases.

The $a_{\rm sym}/T$ of FFs produced in the 80 A MeV ^{60}Ni+^{12}C reactions with $b_{\max}$=1.5, 2 and 7.3 fm are plotted in Fig. 6. For the I=1 fragments in reactions of different $b_{\max}$, $a_{\rm sym}/T$ of the $A<25$ fragments has very little difference, and increases from 8 to 15 almost linearly, while $a_{\rm sym}/T$ of the $A>25$ fragments increases when $b_{\max}$ increases. For the $I=3$ fragments, $a_{\rm sym}/T$ increases as A increases, and the results are similar when $A<35$. For $I>3$ fragments when $b_{\max}$=7.3 fm, $a_{\rm sym}/T$ increases as A increases tardily. As the impact parameter in some sense represents temperature and the violence of the collisions, the $a_{\rm sym}/T$ results indicate that it decreases when the collisions are more violent and of higher temperature, which also is coincident with the conclusion of Ref. [35].

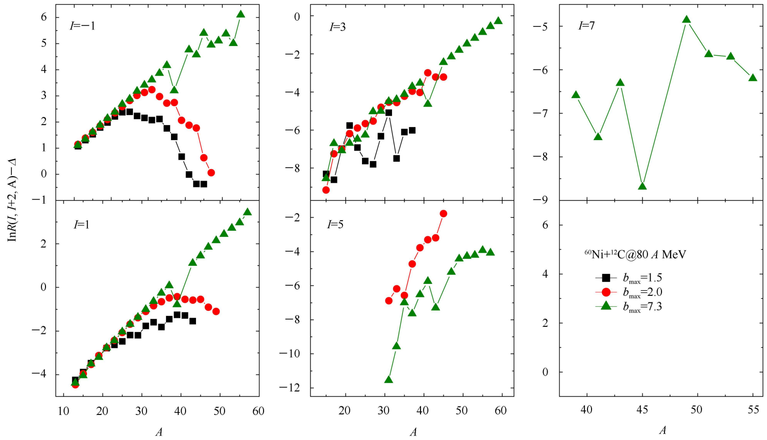

Fig. 5. The isobaric yield ratios (in the form of $\ln R(I,I+2,A)-\Delta$) of the final fragments produced by the 80 A MeV ^{60}Ni+^{12}C reactions with different limitations on the impact parameter. The IYRs in reactions with $b_{\max}$=1.5, 2.0 and 7.3 fm are plotted as squares, circles, and triangles, respectively.

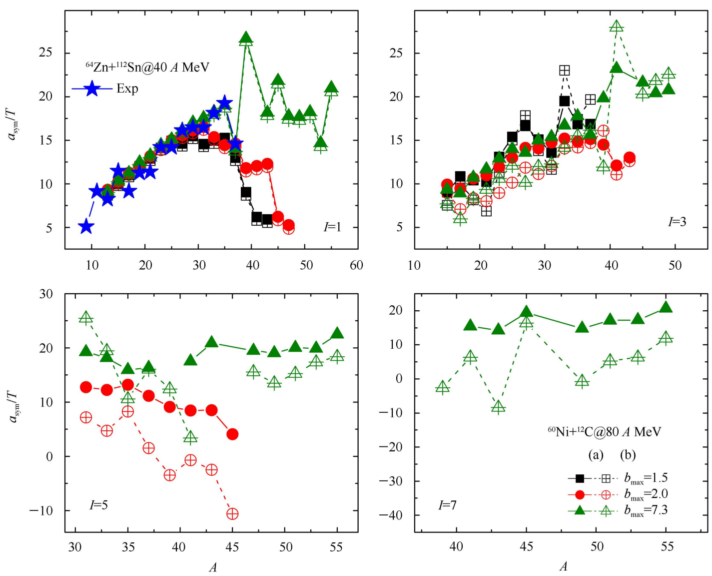

Fig. 6. (color online) The $a_{\rm sym}/T$ of FFs produced in the 80 A MeV ^{60}Ni+^{12}C reactions with $b_{\max}$=1.5, 2 and 7.3 fm. (a) and (b) represent the results using Eqs. (6) and (7), respectively.

Comparing the $a_{\rm sym}/T$ results of fragments in Figs. 3 and 6 using Eqs. (6) and (7), of which taking different IYRs as the reference [represented by (a) and (b) in the figures], either for PFs or FFs, the results of (b) are lower than those of (a) except the $I=1$ fragments. The difference between (a) and (b) becomes larger as I increases, which indicates the reference IYR has notable influence on the resultant results. For the mirror nuclei, the $[(\mu_{\rm n}-\mu_{\rm p})+2a_{\rm c}/A^{1/3}]/T$ terms are smaller than those of the neutron-rich isobars. For the neutron-rich fragments, the results of taking the IYRs of mirror nuclei as reference are larger than those of the $(I-2)$ IYR.

It should be pointed out that the symmetry energy for neutron-rich nuclei should include a surface-symmetry energy term, and the the symmetry-energy coefficient is related to the surface-symmetry energy and volume-symmetry energy by $4a_{\rm sym}/A=b_{\rm v}/A-b_{\rm s}/A^{4/3}$ [37, 38], where $b_{\rm v}$ and $b_{\rm s}$ are the volume-symmetry energy and the surface-symmetry energy coefficients, respectively. Here the correlation is written as $a_{\rm sym}/T=b_{\rm v}/(4T)$–$b_{\rm s}/(4A^{1/3}T)$. Using this correlation, the $a_{\rm sym}/T$ of the $I=1$ and $I=3$ fragments are fitted. $b_{\rm v}$ and $b_{\rm s}$ are obtained. The results are plotted in Fig. 7. For the $I=1$ fragments, $R_{\rm s/v}(\equiv b_{\rm s}/B_{\rm v})$ is 1.887. While for the $I=3$ fragments, $R_{\rm s/v}$ is 2.611. The extracted $R_{\rm s/v}$ for the $I=1$ and $I=3$ fragments is in the normal range of the results of Refs. [37, 38]. For the more neutron-rich fragments, $b_{\rm v}$ and $b_{\rm s}$ are unable to be extracted due to very little data.

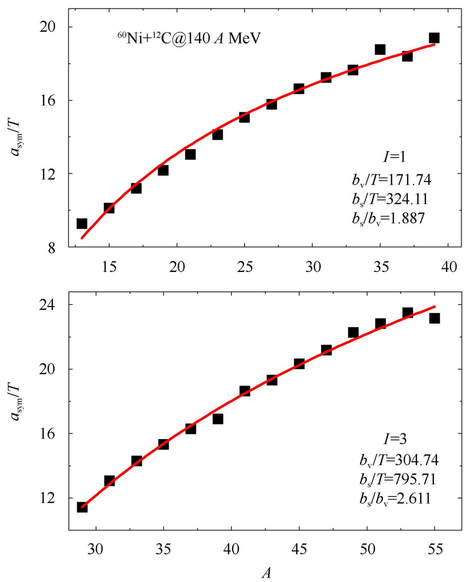

Fig. 7. (color online) The fitting of $a_{\rm sym}/T$ of the $I=1$ and $I=3$ fragments using a correlation $a_{\rm sym}/(T)$=$b_{\rm v}/(4T)$−$b_{\rm s}/(4A^{1/3}T)$.

4 Summary

In summary, using the isobaric yield ratio method, the cross sections of fragments produced in the ^{64}Ni+^{12}C at 80 A and 140 A MeV and with different impact parameter at 80 A MeV, which are calculated using the statistical abrasion-ablation model, are analyzed to extract the coefficient of symmetry energy of fragments. The incident energy influences the $a_{\rm sym}/T$ of final fragments very little. It's found that $a_{\rm sym}/T$ of fragments with the same I increases when A increases, while $a_{\rm sym}/T$ of isobars decreases when A increases. The $a_{\rm sym}/T$ of prefragments is smaller than that of the final fragments, and the $a_{\rm sym}/T$ of fragments in small impact parameters is smaller than that of the larger impact parameters in reactions, which suggests that $a_{\rm sym}/T$ decreases as T increases. The choice of the reference IYRs is found to also have influence on the extracted $a_{\rm sym}/T$ of fragments, especially the more neutron-rich fragments. The surface-symmetry energy and the volume-symmetry energy coefficients are obtained from the extracted $a_{\rm sym}/T$ of fragments, and $R_{\rm s/v}$ of the $I=1$ and $I=3$ fragments agree with the theoretical results.

We wish to thank Dr. HUANG Mei-Rong, at Institute of Modern Physics (Chinese Academy of Sciences), for providing us with their measured results and her helpful discussion.

References

1 Danielewicz P, Lacey R, Lynch W G. Science, 2002, **298**: 1592
2 Lattimer J M, Prakash M. Phys. Rep., 2000, **333**: 121; Astrophys. J, 2001, **550**: 426; Science, 2004, **304**: 536
3 Baran V, Colonna M, Greco V et al. Phys. Rep., 2005, **410**: 335.
4 Steiner A W, Prakash M, Lattimer J M et al. Phys. Rep., 2005, **411**: 325
5 Fuchs C. J. Phys. G: Nucl. Part. Phys., 2008, **35**: 014049
6 LI B A, CHEN L W, Ko C M et al. Phys. Rep., 2008, **464**: 113
7 MA Y G, Natowitz J B, Wada R et al. Phys. Rev. C, 2005, **71**: 054606
8 XU H S, Tsang M B, LIU T X et al. Phys. Rev. Lett., 2000, **85**: 716
9 Henzlova D, Botvina A S, Schmidt K H et al. J. Phys. G: Nucl. Part. Phys., 2010, **37**: 085010
10 Danagulyan A S, Balabekyan A R, Hovhannisyan G H. Phys. Atomic Nuclei, 2010, **73**: 81
11 MA C W, FU Y, FANG D Q et al. Int. J. Mod. Phys. E, 2008, **17**: 1669
12 ZHOU P, TIAN W D, MA Y G et al. Phys. Rev. C, 2011, **84**: 037605
13 FANG D Q, MA Y G, ZHONG C et al. J. Phys. G: Nucl. Part. Phys., 2007, **34**: 2173
14 HUANG M, CHEN Z, Kowalski S et al. Phys. Rev. C, 2010, **81**: 044620
15 MA C W, WANG F, MA Y G et al. Phys. Rev. C, 2011, **83**: 064620
16 MA C W, PU J, WANG S S, WEI H L. Chin. Phys. Lett., 2012, **29**: 062101
17 Minich R W, Agarwal S, Bujak A et al. Phys. Lett. B, 1982, **458**: 267c
18 Hirsch A S, Bujak A, Finn J E, Gutay L J, Minich R W, Porile N T, Scharenberg R P, Stringfellow B C, Turkot F. Phys. Rev. C, 1984, **29**: 508
19 MA C W, WEI H L, LIU G J et al. J. Phys. G: Nucl. Part. Phys., 2010, **37**: 015104
20 WEI H L, MA C W. Acta Phys. Sin., 2010, **59**: 5364 (in Chinese)
21 MA C W, WANG S S. Chin. Phys. C (HEP & NP), 2011, **35**: 1017
22 FANG D Q, SHEN W Q, FENG J et al. Phys. Rev. C, 2000, **61**: 044610
23 MA C W, WEI H L, FU Y et al. Phys. Rev. C, 2009, **79**: 034606
24 von Weizsäcker C F. Z. Phys., 1935, **96**: 431
25 Bethe H A. Rev. Mod. Phys., 1936, **8**: 82
26 Green A E S, Edwards D F. Phys. Rev., 1953, **91**: 46
27 Brohm T, Schmidt K H. Nucl. Phys. A, 1994, **569**: 821
28 Gaimard J J, Schmidt K H. Nucl. Phys. A, 1991, **531**: 709
29 MA C W, WEI H L, LI Y Q. Int. J. Mod. Phys. E, 2010, **19**: 1545
30 MA C W, WEI H L, YU M. Phys. Rev. C, 2010, **82**: 057602
31 MA C W, FU Y, FANG D Q et al. Chin. Phys. B, 2008, **17**: 1216
32 FANG D Q, MA Y G, CAI X Z et al. Phys. Rev. C, 2010, **81**: 047603
33 MA C W, WEI H L, WANG J Y et al. Chin. Phys. B, 2009, **18**: 4781
34 CAI X Z, FENG J, SHEN W Q et al. Phys. Rev. C, 1998, **58**: 572
35 DE J N, Samaddar S K. Phys. Rev. C, 2012, **85**: 024310
36 WANG J, Wada R, Keutgen T et al. Phys. Rev. C, 2005, **72**: 024603
37 Danielewicz P. Nucl. Phys. A, 2003, **727**: 233
38 MEI H, HUANG Y, YAO J M, CHEN H. J. Phys. G: Nucl. Part. Phys., 2012, **39**: 015107; and the reference therein